DOI https://doi.org/10.30525/978-9934-26-329-3-7

BASED ON THE COMPTON EFFECT CONTROL OF HIGH-TEMPERATURE SYNTHESIS OF SOLID SOLUTIONS $Li_yNi_{2-y}O_2$

Mikhailov I. F., Mikhailov A. I.

INTRODUCTION

In rechargeable lithium batteries, nickel is used in the form of oxide, in the crystalline structure of which lithium ions are intercalated to produce layered nickel oxide $LiNiO_2$. Structural studies of $Li_yNi_{2-y}O_2$ solid solutions have been the subject of many works. P. Kalyani et al.[1] showed that, in an ideal stoichiometric $LiNiO_2$, cations Li^+ and Ni^{3+} are arranged along the (111) direction of a cubic rock salt-type lattice, which gives a 2-dimensional layered structure, isostructural with α-$NaFeO_2$. The review of M. Bianchini[2] systematized structural studies of the layered structure formation for the isothermal phase diagram of $LiO_2 – NiO – O(1/2\ O_2)$. P. Barton et al.[3] showed that when the phase space point moves from the NiO top to $LiNiO_2$, the lattice constant of a cubic lattice decreases with increasing of y content in $Li_yNi_{2-y}O_2$. At $y = 0.62$, the rock salt structure transforms to layered structures (α-$NaFeO_2$ type). The $(003)_{hex}$ line ($2\theta \approx 18.63$ deg), which is forbidden for the fcc lattice, appears on the diffraction pattern, which indicates a partial ordering in the cation layers and the beginning of the distortion of the cubic lattice to hexagonal. The peak (003) appears due to diffraction of the layered structure of rock salt $R\bar{3}m$, while the peak (104) arises from diffraction of both the layered and cubic structures of rock salt (P. Kalyani et al.)

Ohzuki et al.[4] evaluated the quality of synthesized $LiNiO_2$ by measuring the integrated intensities of the (003) and (104) peaks and concluded that a decrease in the $I_{(003)}/\ I_{(104)}$ ratio indicates the formation of the cubic structure of $LiNiO_2$ due to the displacement of nickel ions into the lithium layer. According to these authors, samples with the $I_{(003)}/\ I_{(104)}$ ratio from 1.32 to 1.38 demonstrate electrochemical activity. The empirical criterion for deviation from stoichiometry of $LiNiO_2$ can be the ratio $(I_{(006)} + I_{(102)})/\ I_{(101)}$ (M. Bianchini); for a stoichiometric sample, this ratio is < 0.41. Most

[1] P. Kalyani, N. Kalaiselvi, Sci. Technol. Adv. Mater, 2005, 6(6), pp. 689-703. https://doi.org/10.1016/j.stam.2005.06.001

[2] M. Bianchini, Angew. Chem. Int. Ed., 2018, 58(31). DOI: 10.1002/anic.201812472

[3] P. Barton, D. Premchand, P. Chater, R. Seshadri, M. Rosseinsky, Chem. Euro. J. 2013, 19, 14521. https://doi.org/10.1002/chem.201301451

[4] T. Ohzuki, A. Veda, M. Nagayam, Electrochem. Acta, 1993, 38 p. 1159.

researchers report difficulties in obtaining $LiNiO_2$ with a controlled deviation from stoichiometry.

Thus, the main problem remains the preparation of $Li_yNi_{2-y}O_2$ solid solutions with a given level of ordering. However, the final state of the system after solid-phase synthesis is determined not only by the phase diagram, but also by the kinetics of the processes occurring during the synthesis according to S. Deng et al.[5].

The kinetics of $LiNiO_2$ synthesis in the temperature range of 650 to 850°C was considered by Chung-Hsin Lu et al.[6] using the reaction:

$$NiO + \frac{1}{2}Li_2CO_3 + \frac{1}{4}O_2 = LiNiO_2 + \frac{1}{2}CO_2 \uparrow \quad (1)$$

The degree of transformation of the reaction was determined by the change of mass of solid-phase components. According to calculations by atomic masses, with a complete reaction, the mass of the sample should be reduced by 12.54%. Based on this weight loss, kinetic curves were plotted and the diffusion-controlled mechanism of the process with activation energy 76.1 $kJ \cdot mol^{-1}$ for the reaction (1) was determined. However, in more recent works (S. Deng et al., V. Kaplan et al.[7], D. Gonzalez-Varela et al.[8]) partial decomposition of $LiNiO_2$ obtained by the reaction (1) was established, which results in a sharp mass loss at the synthesis temperature $T > 700$°C. This indicates, the mass loss cannot be described only be the reaction (1); and for mass balance, along with the mass loss, an additional control of the composition of the final solid product is required.

It is a priori clear that at least three processes are involved in solid-phase synthesis (B. Delmon [9]): consumption of the phase of a lithium source; delivery of lithium to NiO grains and formation of a disordered solid solution with a rock salt lattice; ordering lithium in a lattice with the formation of a layered structure. Each of these processes can determine the limiting stage of solid-phase synthesis and, ultimately, determine the final state of $Li_yNi_{2-y}O_2$. That is why, to develop a technology for producing $Li_yNi_{2-y}O_2$ solutions with a controlled deviation from stoichiometry, quantitative characteristics of the kinetics of these processes are necessary.

---

[5] S. Deng, L. Xue, Y. Li, Z. Lin, W. Li, Y. Chen, T. Lei, J. Zhu, J. Zhang, J. Fuel Cell Sci. Technol., 2019, 16(3). DOI: 10.1115/1.4042552

[6] Chung-Hsin Lu, Lee Wei-Cheng, J. Mater. Chem, 2000, 10, pp. 1403-1407. https://doi.org/10.1039/A909130K

[7] V. Kaplan, E. Wachtel, I. Lubomirsky, J. Chem. Thermodyn, 2011, 43(11), pp. 1623-1627. https://doi.org/10.1016/j.jct.2011.05.020

[8] D. Gonzalez-Varela, H. Pfeiffer B. Alcántar-Vázquez, Journal of Materiomics, 2018, 4(1), pp. 56-61. DOI: 10.1016/j.jmat.2017.12.004

[9] B. Delmon, Introduction a la Cinetique Heterogene. Edition Technip. 7 Rue Nelaton, Paris, 1969, p. 540.

The aim of this work was to study the basic physicochemical processes that occur during solid-phase synthesis of $Li_yNi_{2-y}O_2$ solid solutions. To achieve this aim it is necessary: (1) to construct the kinetic dependences of the consumption of a lithium source, an increase in the total lithium content in the $Li_yNi_{2-y}O_2$ solid solution and an increase in the degree of lithium ordering in a layered structure; (2) to determine the dependence of the rates of these processes on temperature and excess lithium; (3) to construct a diagram «composition – degree of ordering» to control deviations from the structure of equilibrium phases.

1. Determination of the lithium content from the ratio of the intensities of the Compton and Rayleigh scattering peaks

The measurement of the ratio of the peaks of incoherent (Compton) and coherent (Rayleigh) scattering was proposed by Compton to identify elements with a small atomic number. Unlike all known X-ray methods, the sensitivity of this method increases with decreasing atomic number of the scatterer material; thus, it can be used to identify light elements up to hydrogen. Recently, this method was used for measurements of carbon in solid fuel (I.F. Mikhailov et al.[10]) and an effective atomic number of oxides (P. Duvauchell[11]). P. Duvauchell showed that the ratio of the scattering peaks is practically independent on the structure of the scatterer and completely determined by its composition. Therefore, this ratio is conveniently used to certify the effective atomic number of the initial and final mixtures of reagents to determine the mass balance of the chemical reaction.

The Compton and Rayleigh scattering of X-rays by a set of atoms does not depend on the structural state of the system, but is determined only by the atomic concentrations of the components. The composition of the mixture of two phases Li_2CO_3 and $Li_yNi_{2-y}O_2$ can be certified by the ratio of the intensities of Compton and Rayleigh scattering I_C/I_R in accordance with the methodology of I.F. Mikhailov et al.. In works of (I.F. Mikhailov et al. and P. Duvauchell), it was shown that the ratio I_C/I_R for a mixture of multicomponent substances can be represented by the formula

$$\frac{I_C}{I_R} = \frac{\sum_{i=1}^{m} n_i S\left(Z_i, \frac{\sin\theta}{\lambda}\right)}{\sum_{i=1}^{m} n_i f^2\left(Z_i, \frac{\sin\theta}{\lambda}\right)}, \quad (2)$$

where 2θ and λ is scattering angle and wavelength; $S\left(Z_i, \frac{\sin\theta}{\lambda}\right)$ is the function of incoherent scattering; and $f\left(Z_i, \frac{\sin\theta}{\lambda}\right)$ is the atomic form-factor for the

[10] I.F. Mikhailov, A.A. Baturin, A.I. Mikhailov, S.S. Borisova, L.P. Fomina, Rev. Sci. Instrum, 2018, 89(2), 023103, DOI:10.1063/1.4993101

[11] P. Duvauchell, Nucl. Instrum. Methods Phys. Res., Sect. B, 1999, 155, pp. 221-228

chemical element with atomic number Z_i; n_i is the number of atoms of the *i*-th sort.

As it follows from Eq. (2), the intensity of Compton scattering is determined by the sum of functions of incoherent scattering of atoms, while for Rayleigh scattering, it is the sum of squares of atomic form-factors. These sums are similar to the sum of atomic masses when calculating the total molecular mass $M = \sum_{i=1}^{m} n_i A_i$. Therefore, a change in the I_C/I_R ratio may be a measure of a change in molecular mass as a result of a chemical reaction. Compare the sensitivity of two methods for determination of a change in molecular mass: (i) by the measurement of masses of the initial and final products and (ii) by measurement of the I_C/I_R ratio on the example of the reaction (1). According to Chung-Hsin Lu et al., the relative mass change of solid products at the completed reaction is 12.54 %. At this, the I_C/I_R ratio changes from

$$\frac{S_{Ni}+S_O+S_{Li}+\frac{1}{2}\cdot S_C+\frac{3}{2}\cdot S_O}{f_{Ni}^2+f_O^2+f_{Li}^2+\frac{1}{2}\cdot f_C^2+\frac{3}{2}\cdot f_O^2} \text{ to } \frac{(S_{Li}+S_{Ni}+2S_O)}{(f_{Li}^2+f_{Ni}^2+2f_O^2)}.$$

For $\frac{\sin\theta}{\lambda}$ = 1.08 Å^{-1}: f_{Li} = 0.277; f_C = 1.033 f_O = 1.314; f_{Ni} = 6.584; S_{Li} = 2.942; S_C = 5.434; S_O = 7.002; S_{Ni} = 20.08 (J.H. Hubbell[12]), and the relative change in the ratio $\Delta\left(\frac{I_C}{I_R}\right)/\left(\frac{I_C}{I_R}\right)$ =11.83%.

Thus, the sensitivity to the change of molecular mass of the solid product is almost similar for these two methods. However, the measurement of Compton scattering is possible in the *in situ* experiments along with XRD, that allows us to plot kinetic curves of molecular mass decrease (by the ratio of the scattering peaks) and, simultaneously, obtain curves of an increase in the lithium content in the solid solution (from the change in the lattice parameter).

For a mixture of chemical compounds, it is convenient to write (2) through their molecular weight *M* and mass fraction *W* (I.F. Mikhailov et al.):

$$\frac{I_C}{I_R} = \frac{\sum_i \frac{W_i}{M_i} \sum_j n_j s_j}{\sum_i \frac{W_i}{M_i} \sum_j n_j f_j^2}. \quad (3)$$

Equation (3) allows us to determine the mass fraction of the residual Li_2CO_3 phase from the experimental I_C/I_R values using a calibration with reference mixtures. The calibration for the experimental determination of the I_C/I_R value from relation (3) was performed using reference mixtures of Li_2CO_3 and NiO subjected to heat treatment to remove moisture. In addition, single-phase samples of solid solutions with a lithium content of $y \approx 0.92$ were used.

[12] J.H. Hubbell, Phys. Chem. Ref. Data. 1975, 4, p. 471 https://doi.org/10.1063/1.555523

2. Kinetics of solid-phase synthesis of $Li_yNi_{2-y}O_2$ solid solutions

Further, we will discuss only the results of the studies, since the sample preparation process and the measurement technique are discussed in detail in the work of Mikhailov I.F., Gabielkov S.V. et al.[13]. In the diffraction patterns of the samples subjected to heat treatment at a temperature of 650°C, reflections of the Li_2CO_3 component and the $Li_yNi_{2-y}O_2$ solid solution with the rock salt structure (M. Bianchini) are observed (Fig. 1). With an increase in the heat treatment temperature and an increase in its duration, the reflections of Li_2CO_3 significantly weaken and completely disappear at the temperature of 850°C (Fig. 2). The decrease in the intensity of Li_2CO_3 reflections with an increase in the duration of heat treatment indicates a decrease in the residual amount of this component of the reaction. All reflections of a solid solution with a rock salt cubic lattice are shifted toward large diffraction angles. This shift corresponds to an increase in y in the solid solution. Upon reaching $y \approx 0.55$, the diffraction patterns show a reflection (003) at an angle of $2\theta \approx 18$ degrees. This indicates a transition to a two-dimensional layered structure (α-$NaFeO_2$ type). The intensity of the reflection (003) increases with increasing temperature and duration of the heat treatment, which is consistent with the results of several works (P. Kalyani et al., M. Bianchini). A similar two-phase system Li_2CO_3 – $Li_yNi_{2-y}O_2$ was also observed after heat treatment at a temperature of 750°C. Long exposure (from 96 to 144 hours) at a temperature of 850°C allowed us to obtain almost single-phase samples, i.e. only reflections of $Li_yNi_{2-y}O_2$ are present on the diffraction pattern (Fig. 2).

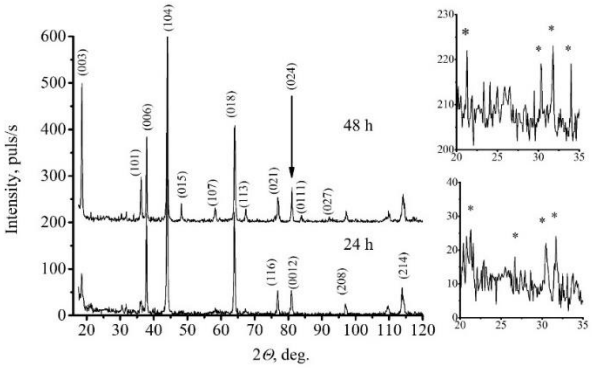

Fig. 1. Diffraction patterns of lithium nickelate nano-powder (heat treatment at T = 650 ºC: bottom – 24 h; top – 48 h); stars (∗) denote reflections of lithium-containing phases without nickel

[13] Mikhailov I.F., Gabielkov S.V., Mikhailov A.I., Surovitskiy S.V., Rev. Sci. Instrum., 2022, 93, 084102

In the reflection groups of (006), (012) (2θ = 38 deg), (018), (110) (2θ = 64 deg), and (1112), (214) (2θ = 114.5 deg) clear separation of reflections is observed (inset in Fig. 2). The values of a = 0.2885 nm and c/a = 4.917 were determined from the positions of these peaks, which corresponds to the value y = 0.918. Using a prolonged exposure, it was possible to obtain samples that, according to the c/a ratio, corresponded to the lithium content y from 0.918 to 0.946. The intensity ratio $I_{(006)}/I_{(101)}$ for these samples lies in the range from 0.6 to 0.9, which indicates a deviation from stoichiometry (review of M. Bianchini).

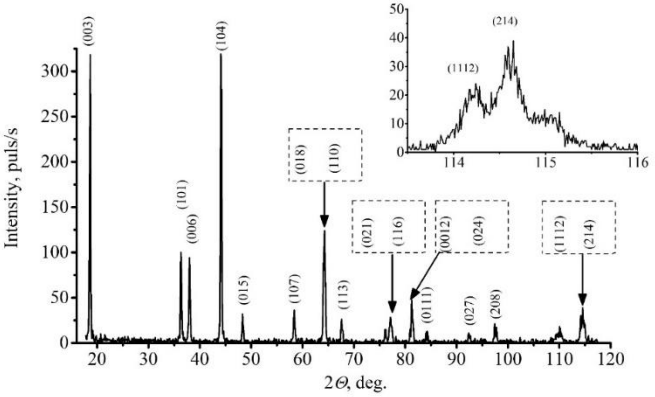

Fig. 2. Diffraction pattern of lithium nickelate nanopowder after heat treatment at 850°C for 144 h. The inset shows the separation of reflections (1112) and (214)

In view of the foregoing, the reaction of the formation of a $Li_yNi_{2-y}O_2$ solid solution during the interaction of NiO and Li_2CO_3 can be represented as:

$$2\cdot(2\text{-}y)\ NiO + y\cdot Li_2CO_3 + 0.5\ O_2 = 2\ Li_yNi_{2-y}O_2 + y\cdot CO_2\uparrow. \qquad 4)$$

Let us move to compilation of a mass balance. We consider the Li_2CO_3 – $Li_yNi_{2-y}O_2$ system is subjected to heat treatment. At time t, the Li_2CO_3 content is $W(t)$ % mass, and for the $Li_yNi_{2-y}O_2$ phase it is, respectively, (100−$W(t)$) % mass. Then the equation of mass balance in the transition from time t_1 to t_2:

$$\frac{W(t_1)}{M_{Li_2CO_3}}\cdot Li_2CO_3 + \frac{100-W(t_1)}{M_{Li_yNi_{2-y}O_2}}\cdot Li_yNi_{2-y}O_2 + O_2 \rightarrow \frac{W(t_2)}{M_{Li_2CO_3}}\cdot Li_2CO_3 + \frac{100-W(t_2)}{M_{Li_{y'}Ni_{2-y'}O_2}}\cdot Li_{y'}Ni_{2-y'}O_2 + CO_2\uparrow, \qquad (5)$$

where $M_{Li_2CO_3}$=73.9 is the molecular mass of Li_2CO_3, and $M_{Li_yNi_{2-y}O_2} = y \cdot A_{Li} + (2-y)A_{Ni} + 2A_O = 149.4 - 51.8 \cdot y$ is the molecular mass of the solid solution.

Table 1

The ratio of the Compton and Rayleigh scattering intensities I_C/I_R, the atomic fraction y of lithium in the $Li_yNi_{2-y}O_2$ solid solution and the content of residual Li_2CO_3, W, (% mass) depending on the heat treatment time t at different temperatures T = 650°C

t, h	2.25M			3M			6M			
	I_C/I_R	y	W, (% mass)	I_C/I_R	y	W, (% mass)	t, h	I_C/I_R	y	W, (% mass)
1	0.261	0.246	26.7	0.358	0.206	48.5	1	0.490	0.261	66.0
4	0.263	0.333	26.1	0.361	0.340	47.8	15	≈0.50	0.561	65.0
27	0.263	0.621	20.8	0.348	0.659	41.0	24	0.501	0.734	62.0
41	0.260	0.734	16.9	0.347	0.742	39.5	39	0.504	0.758	62.0
51	0.245	0.750	11.0	0.344	0.765	38.0	48	0.491	0.758	60.5

T = 750°C

t, h	2.25M			3M		
	I_C/I_R	y	W, (% mass)	I_C/I_R	y	W, (% mass)
1	0.284	0.374	31.2	0.350	0.333	46.0
3	0.284	0.582	27.5	0.339	0.438	42.5
23	0.243	0.919	5.0	0.315	0.802	30.5
48	0.245	1.00	3.0	0.304	0.930	24.5

The mass balance will be controlled by equation (4). $W(t_1)$ is determined by measuring the ratio of the peaks of Compton and Rayleigh scattering I_C/I_R (Eq.(3)), and the content of lithium y in the solid solution is estimated by d_{208} (Table 1). Let us analyze the data in Table. At a temperature of 650°C, there is a slight decrease in the I_C/I_R ratio with the heat treatment time – within 7% of the measured value. This decrease is associated only with the removal of the reaction product CO_2 from the reaction zone, but not with the removal of lithium from the mixture. Indeed, in accordance with (4), to increase the lithium content in the solid solution from y = 0.246 (T = 650°C, 2.25 M, t = 1 hour) to y = 0.750 (T = 650°C, 2.25 M, t = 51 hours), it will take (0.75–0.246) moles of Li_2CO_3, which corresponds to a decrease in its content in the mixture by 16% mass. This result gives the difference between the measured values of the residual Li_2CO_3 content: ΔW = 26.7 – 11.0 = 15.7%. Thus, no significant loss of lithium-containing substances at a temperature of 650°C was detected.

An increase in the heat treatment temperature to 750°C leads to a 15% decrease in the I_C/I_R ratio after exposure for 48 hours. According to the previous estimate, such a change cannot be explained only by the consumption of Li_2CO_3 in the formation of a solid solution. As can be seen from the table,

the consumption of the source mass W increases at least two times as compared with the results at T = 650 ° C. This indicates a sharp increase in lithium removal, when the heat treatment temperature exceeds 700-720°C. Uncontrolled lithium release during high-temperature heat treatment leads to a violation of the mass balance and can change the kinetics of synthesis.

Thus, in the solid-phase synthesis of $Li_yNi_{2-y}O_2$, three processes occur: (1) consumption of a lithium source (taking into account leaving the reaction zone); (2) disordered saturation of the solid solution with lithium, which can be characterized by a change in its interplanar distance; (3) ordering in the arrangement of lithium atoms with the formation of a layered structure, which can be characterized by the intensity of the (003) reflection. The kinetics of each of these processes can determine the limiting stage of the solid-phase synthesis. Along with the phase diagram, it is the limiting stage of the process that determines the final synthesis product and should be taken into account when developing the technology. To determine the kinetics of these three processes, we consider the dependences of structural characteristics on temperature, heat treatment time, and excess lithium in the reagent mixture.

2.1. The kinetics of expenditure of the lithium source

Let us consider the change of the rate of the Li_2CO_3 source expenditure depending on the lithium excess in the initial mixture. First of all, we note that the greater the excess of Li_2CO_3 in the initial mixture, the larger the size of blocks in this phase (Table 2). The fitting of the values of residual Li_2CO_3 depending on the thermal treatment time, $W(t)$, at the temperature of 650 °C (Table 1) results in linear equations $W(t) = (k \cdot t + b) \times 100\%$mas (Table 2) (Fig 3, curves 1, 2). This dependence is typical for zero order reactions.

Table 2

The block size in the Li_2CO_3 phase and coefficients k (h– 1) and b of the regularization solution according to data of Table 1. (W is in relative units)

Excess Li_2CO_3	L, nm	k, h^{-1}	b
2.25M	50	-0.00292	0.276
3M	80	-0.00217	0.483
6M	≈100	-0.00116	0.660

As it is seen from Table 2, as the excess of Li_2CO_3 increases, the block size in this phase significantly increases, while the rate of its expenditure decreases. Therefore, in solid-phase synthesis, i.e. at a temperature below the melting point of Li_2CO_3 (720 °C), one should strive for the smallest block size, and consequently, for the minimum excess of the phase – lithium source.

(3M)

At the temperature 750 °C, i.e. above the Li_2CO_3 melting point, the dependence $W(t)$ is not a linear function (Fig 3, curves 3, 4). The fitting of the data from Table 1 leads to the relations:

$W(t) = 0.33 \cdot \exp(-0.06 \cdot t)$ for the 2.25M of the Li_2CO_3 excess at $L = 60$ nm

$W(t) = 0.46 \cdot \exp(-0.016 \cdot t)$ for the 3M of the Li_2CO_3 excess at $L = 90$ nm.

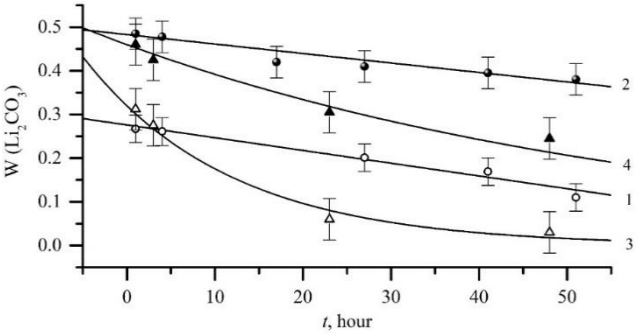

Fig. 3. Mass fraction of residual Li2CO3 depending on the heat treatment time at different temperatures

1 – T = 650°C (2.25M); 2 – T = 650°C (3M); 3 – T =750°C (2.25M); 4 – T =750°C This dependence is typical for first-order reactions, characteristic of the decomposition of molecules. It is important to note, that in this case as well, the rate of the reaction significantly increases with decreasing the block size *L*. When the synthesis temperature passes through the melting point (720 °C) of Li_2CO_3, the reaction order of the source consumption changes. Therefore, it is difficult to determine the activation energy of the source consumption from data of Table 1.

2.2. Kinetic curves of lithium content in the solid solution – a reaction product

The dependences of the lithium content in the solid solution, *y*, on the time of heat treatment at a temperature of 650°C are almost identical for different excess of lithium in the initial mixture (Fig. 4, curve 1). Kinetic curves in the initial and middle parts are well described by the function $y(t)=const+(k \cdot t)^{1/2}$. This dependence indicates that the process is limited by diffusion rather than boundary kinetics (B. Delmon). However, with a long heat treatment time $t = 50$ hours, all the curves, regardless of the amount of residual Li_2CO_3, asymptotically converge to the same value $y = 0.76 \pm 0.01$. Such a halt in the

growth of the *y(t)* curve is not related to the depletion of the lithium source (Table 1), but it may well be due to the phase diagram. The enthalpy of formation of $Li_yNi_{2-y}O_2$ at $y > 0.7$ sharply increases (Hena Das[14]), which can cause an increase in the thermodynamic potential of the reaction and the halt in the reaction of formation of the solid solution. It is noteworthy that the asymptote value is close to the *y* value for the equilibrium phase $Li_{0.75}Ni_{1.25}O_2$. An increase in temperature to 750°C does not change the diffusion nature of the dependence (Fig. 4, curve 2), but is accompanied by an increase in the slope of the curve and leads to an increase in the level of asymptote to $y=0.95\div1$. This value is characteristic of the equilibrium phase of $LiNiO_2$.

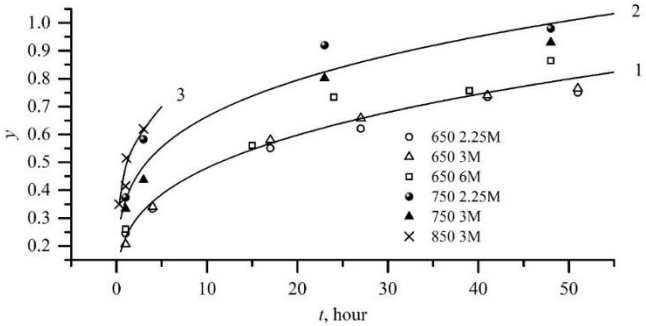

Fig. 4 – Dependence of the lithium content *y* in the $Li_yNi_{2-y}O_2$ solid solution on the time of heat treatment at various temperatures T: 1 – 650°C; 2 – 750°C; 3 – 850°C

In the beginning stage, the process of $Li_yNi_{2-y}O_2$ formation (according to the reaction (4) is related with Ni diffusion from NiO nano-particles as well as by counter Li diffusion from Li_2CO_3 (Hena Das). A feature of NiO is that the Ni diffusion coefficient is two orders of magnitude lower, than that of vacancies in this substance (T. Karakasidis and M. Meyer[15]). At this, the diffusion coefficients of Ni and Li are practically the same. For this reason, the diffusion process of lithium saturation of NiO particles is complex and leads to the formation of vacancy complexes in the final product (Hena Das). Diffusion of lithium, nickel and vacancies occurs inside solid NiO particles regardless of the state (solid or liquid) of the lithium source (Li_2CO_3). This is probably the reason why the kinetic curves obtained at the synthesis

[14] Hena Das, Chem. Mater, 2017, 29(18) pp. 7840-7851 https://doi.org/10.1021/acs.chemmater 7b02546

[15] T. Karakasidis and M. Meyer, Phys.Rev B, 1997, 55(20), pp. 13853-13864

temperature below and above the melting point of Li_2CO_3 (T = 723°C) differ only in numerical coefficients. After a significant amount of $Li_yNi_{2-y}O_2$ is formed, a partial destruction of the solid solution takes place, and in the Li_2CO_3 – $Li_yNi_{2-y}O_2$ quasibinary system, the mutual diffusion occurs which has a complex character and, probably, can be considered using a phenomenology approach (C. D'Agostino[16]).

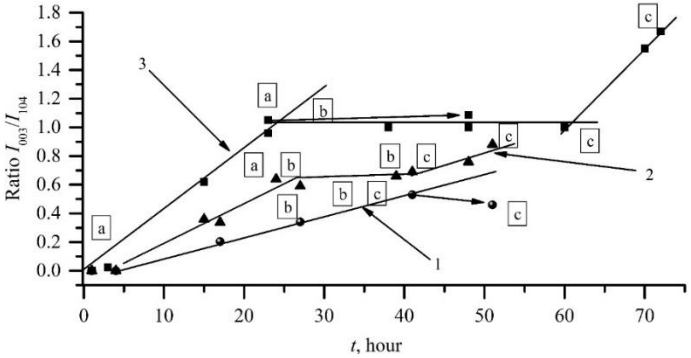

Fig. 5. Dependence of the degree of ordering of lithium (intensity ratio I003/I104) in the lattice of the $Li_yNi_{2-y}O_2$ solid solution on the heat treatment time for various temperatures and excess lithium; (a – a) is the initial heat treatment period; (b – b) is the plateau region; (c – c) is the final period; 1– 650°C, 2,25M; 2 – 650°C, 3M; 3 – 750°C, 3M

However, our experimental data do not allow us to consider this issue in depth. We define the diffusion rate as the derivative $\frac{\partial y(t,T)}{\partial t}$ at a constant temperature T. Then from the Arrhenius equation we get the value of the apparent activation energy of diffusion E_D or otherwise, the thermal increment of diffusion through a solid product (B. Delmon). By fitting the experimental curves 1 and 2 (Fig. 3), the values $k_1 = 0.008 \pm 0.0003$ h^{-1} for T = 650°C and $k_2 = 0.012 \pm 0.001$ h^{-1} for T = 750°C were obtained. Then, for the activation energy, we obtain the value $E = 32 \pm 2$ kJ/mol. The initial portion of the curve in which the disordered solid solution with the rock salt structure dominates is measured in more detail. Here, the k value was fitted for y<0.6 at temperatures T_1= 650°C and T_2= 850°C. From the y change in the disordered solid solution, the values $k_1 = 0.013 \pm 0.0003$ h^{-1}, $k_2 = 0.06 \pm 0.001$ h^{-1} and E = 66 ±2 kJ/mol were obtained.

[16] C. D'Agostino, Chem. Eng. Sci., 2012, 74, pp. 105-113.

Table 3. Intercalation rate constants $\partial\left(\frac{I_{003}}{I_{104}}\right)/\partial t$ (h^{-1}) depending on temperature and excess lithium for various straight sections of the kinetic curve (Fig. 5), as well as the corresponding activation energy, *E*, kJ/mol

T, °C	Intercalation rate constant $\partial\left(\frac{I_{003}}{I_{104}}\right)/\partial t$ (h^{-1})		
	2.25M	3M	
	a – a	a – a	c – c
650	0.012	0.0205	0.014
750	0.043	0.045	0.050
E, kJ/mol	100	62	96

Thus, the character of the dependences *y(t)* is determined by diffusion. The temperature dependence of the rate is weaker than that of the source consumption process. Therefore, an increase in temperature will lead to an outstripping rate of consumption of the lithium source compared to its delivery to the reaction zone and the formation of the solid solution.

2.3. Kinetic curves of the intercalation process

The dependence of the ratio I_{003}/I_{104} on the heat treatment time is strictly linear in a fairly wide time interval, both at a temperature of 650°C (Fig. 5, curves 1, 2) and at 750°C (Fig. 5, curve 3). The linear dependence corresponds to zero-order reactions (B. Delmon). At 650°C, there is an increase in the slope of the straight line with an increase in the excess of lithium (Fig. 4a, curves 1, 2). However, at T = 750°C, such a change could not be detected. All the curves have a latent period of 1 to 7 hours. The latent period decreases with increasing temperature and excess lithium. The presence of the latent period indicates that the beginning of the ordering process is delayed in relation to the process of formation of the solid solution.

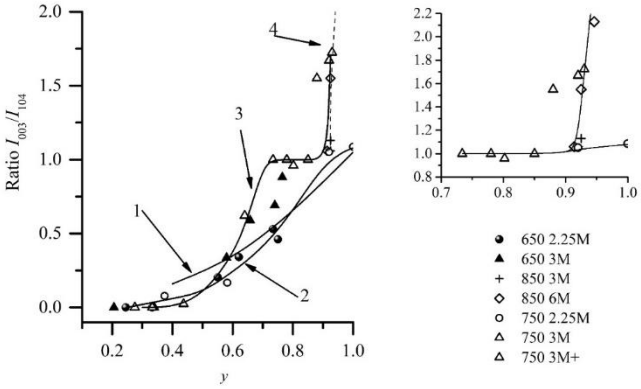

Fig. 6. Diagram 'degree of ordering versus composition y of the solid solution' (experimental values are connected by lines for clarity): 1 – constructed from tabular values of y and the ratio I_{003}/I_{104} for equilibrium phases with a layered structure (I.F. Mikhailov et al.): $Li_2Ni_8O_{10}$ (y = 0.4, I_{003}/I_{104} = 0.16); $Li_{0.68}Ni_{1.32}O_2$ (y = 0.68, I_{003}/I_{104} = 0.337); $Li_{0.75}Ni_{1.25}O_2$ (y = 0.75, I_{003}/I_{104} = 0.573); $LiNiO_2$ (y = 1, I_{003}/I_{104} = 1.05); 2 – experimental dependence for the lithium excess of 2.25M at a synthesis temperature of 650°C (black circle) and 750 ° C (white circle); 3 – experimental dependence for excess 3M lithium at a synthesis temperature of 650°C (black triangle) and 750°C (white triangle); 4 –experimental dependence for excess lithium 3M (cross) and 6M (cross in circle) at a synthesis temperature of 850°C

As can be seen from the table, at a low heat treatment temperature of 650°C, the ordering rate can be increased by increasing the excess of lithium. The activation energy of the ordering process is the same for the initial (*a* – *a*, Fig. 5) and final (*c* – *c*, Fig. 5) heat treatment periods. This value is times higher than the activation energy of the formation of a disordered solid solution (32 and 65 kJ/mol, respectively). The higher the synthesis temperature, the greater the proportion of lithium goes to ordering. The diagram Fig.6 gives a clear representation of the rates of these processes. Curve 1 refers to the equilibrium phases according to the phase diagram of NiO (rock salt) – $LiNiO_2$ (layered). Experimental curve 2 presents the results of measurements of 2.25M series samples with a minimal excess of lithium (W_{Li2CO3} from 3 to 20% mass at $t \geq$ 20 hours, Table 1). Curve 2 is close to the equilibrium curve 1 at y > 0.55, i.e. for layered structures. An increase in the excess of lithium (3M series, W_{Li2CO3} from 20 to 50 %mass, Table 1) leads to a shift in the experimental curve 3 of the diagram relative to the equilibrium

curve 1. In this case, a horizontal section is observed in curve 3 in the y range from 0.74 to 0.92, which, according to the degree of ordering, I_{003}/I_{104}, corresponds to the equilibrium $LiNiO_2$ phase. However, the value y = 1, characteristic of $LiNiO_2$, cannot be achieved. At $y \geq 0.92$, the ratio I_{003}/I_{104} increases sharply, which corresponds to the data of R.V. Moshtev et al[17].

Table 4

The ratio of the axes, c/a, the corresponding values of the lithium content *y* in the $Li_yNi_{2-y}O_2$ solid solution and the degree of ordering $\frac{I_{003}}{I_{104}}$ depending on the excess lithium (3M and 6M) for samples synthesized at a temperature of 850°C with different exposure times

Lithium excess	3M			6M		
t, h	*c/a*	*y*	$\frac{I_{003}}{I_{104}}$	*c/a*	*y*	$\frac{I_{003}}{I_{104}}$
50	4.9214	0.938	1.13	4.9194	0.933	1.06
72	4.9214	0.938	1.13	4.9214	0.938	1.55
97	4.9214	0.938	1.06	4.9245	0.946	2.13

To extend the plateau to $y = 1$, we increased the temperature to 850°C and set two values of the lithium excess, taking into account the increase in its removal from the mixture: 3M corresponded to an excess of lithium-containing phase (probably Li_2O) of not more than 5 %mass, and 6M – to about 30÷50 %mass. It turned out that with insufficient excess of lithium (3M series), it is not possible to experimentally increase the values of *y* (Table 4), and the degree of ordering is close to the equilibrium phase. Even with a significant excess of lithium (6M), the increase in y is negligible, and it is not possible to achieve $y = 1$. Excess lithium at a temperature of 850°C contributes to a sharp increase in the degree of ordering, as expected from the values of the activation energy of the considered processes.

Thus, the movement of the work point along the equilibrium line of the phase diagram (curve 1) can be ensured by monitoring the minimum excess of lithium in comparison to the stoichiometric value specified by the reaction of formation. With an increase in the lithium excess, a «shelf» is observed in the diagram, which corresponds to the $LiNiO_2$ phase in the ordering degree, but the lithium content y does not reach 1. The latter can be related to vacancies in the sublattices (Hena Das). Therefore, it is very important to establish at what stage of the synthesis vacancies are formed: during the formation of the disordered solid solution or its ordering.

[17] R.V. Moshtev, P. Zatilova, V.Menev, A.Sato, J. Power Sources, 1993, 54, p. 329.

3. Determination of the parameters of the process of lithiation-oxidation of NiO in an open system

The process of lithiation-oxidation in an open system is accompanied by the entry of oxygen from the atmosphere into the mixture of solid reaction components, as well as the release of volatile components: Li and CO_2 outside the reaction volume. Depending on the type of chemical reaction and its structural mechanism (the formation of vacancies in the $Li_yNi_{2-y}O_2$ sublattice), the amount of light components in the reagent system changes.

In the previous section, we discussed the results of experimental determination of the figurative point trajectory from XRD and Compton scattering data. In this section, we will consider the theoretical calculation of the trajectory of a figurative point according to a given model of the chemical reaction that characterizes the process. It will be shown that the trajectory of the figurative point differs significantly for different chemical reactions. Fitting the experimental dependence with various model calculations makes it possible not only to establish the type of chemical reaction, but also to determine its quantitative characteristics.

3.1. Theory

Let us consider the basic reaction of the NiO lithiation-oxidation process using the Li_2O compound (or Li_2CO_3 see Eq. (1)) as a source of lithium (H. Migeon et al. [18] S.Pizzini et al.[19]):

$$NiO + \frac{1}{2}Li_2O + \frac{1}{4}O_2 \downarrow = LiNiO_2 \qquad (6)$$

The lithium source is always taken in excess of the reaction stoichiometry. Depending on the source of lithium, in the intermediate case, a $Li_yNi_{2-y}O_2$ solid solution is formed according to one of the reactions:

$$NiO + n \cdot \frac{1}{2} \cdot \frac{y}{(2-y)} Li_2O + \frac{3}{4} \cdot \frac{y}{(2-y)} O_2 \downarrow = \frac{1}{(2-y)} Li_y Ni_{2-y} O_2. \qquad (7)$$

$$NiO + n \cdot \frac{1}{2} \cdot \frac{y}{(2-y)} Li_2CO_3 + \frac{1}{4} \cdot \frac{y}{(2-y)} O_2 \downarrow$$
$$= \frac{1}{(2-y)} Li_y Ni_{2-y} O_2 + \frac{1}{2} \cdot \frac{y}{(2-y)} CO_2 \uparrow.$$

Considering any chemical reaction, one can calculate the change $\frac{I_C}{I_R}$ when moving from left to right side using equation (7) and tables (J.H. Hubbell). In

[18] H. Migeon et al. The Li2O– NiO -O2 system at 670°C, J. Materials Science, 13, 1978, p. 461-466.

[19] S.Pizzini, R.Morlotti, V.Wagner, J.Electrochem.Soc 116(7), 915 (1969)

the initial state in the solid product, Compton and Rayleigh scattering for the initial composition of the mixture $NiO + n \cdot \frac{1}{2} Li_2O$:

$$S_{Ni} + \ n \cdot S_{Li} + \left(n \cdot \frac{1}{2} + 1\right) \cdot S_0 \ ; \ f_{Ni}^2 + n \cdot f_{Li}^2 + \left(n \cdot \frac{1}{2} + 1\right) \cdot f_0^2 \qquad (8)$$

The composition of the mixture of solid products after the reaction can be represented as:

$$\underbrace{Li\left(n - \frac{y}{(2-y)}\right) + O \cdot \frac{1}{2}\left(n - \frac{y}{(2-y)}\right)}_{\text{Unspent original product}} + \underbrace{\frac{y}{(2-y)} Li + Ni + \frac{2}{2-y} O}_{\text{Solid reaction product}}$$

After the reaction, the Compton scattering of the reactant system can be represented as:

$$\underbrace{S_{Li}\left(n - \frac{y}{(2-y)}\right) + \ S_0 \frac{1}{2} \cdot \left(n - \frac{y}{(2-y)}\right)}_{\text{Unspent original product}} + \underbrace{\frac{y}{(2-y)} \cdot S_{Li} + S_{Ni} + \frac{2}{2-y} \cdot S_0}_{\text{Solid reaction product}} =$$

$$= S_{Ni} + n \cdot S_{Li} + \frac{1}{2} n S_0 - \frac{1}{2} \frac{y}{(2-y)} S_0.$$

$\frac{1}{2} n S_0$ – oxygen in the unspent product; $\frac{1}{2} \frac{y}{(2-y)} S_0$ – oxygen in the reaction product.

Compton scattering intensity:

$$I_C = S_{Ni} + n\left(S_{Li} + \frac{1}{2} S_O\right) + \frac{2}{2-y} \cdot S_0 - \frac{1}{2} \frac{y}{(2-y)} S_0 = S_{Ni} + S_O + n\left(S_{Li} + \frac{1}{2} S_O\right) + \frac{1}{2} \frac{y}{(2-y)} S_0 \qquad (9)$$

Similarly for Rayleigh scattering:

$$I_R = f_{Ni}^2 + n\left(f_{Li}^2 + \frac{1}{2} f_O^2\right) + \frac{2}{2-x} \cdot f_O^2 - \frac{1}{2} \frac{y}{(2-y)} f_O^2 = f_{Ni}^2 + f_O^2 + n \qquad (10)$$

As a result, for the ratio I_C / I_R we get the dependence on *y*:

$$\frac{I_c}{I_R} = \frac{a_0 + a_1 n + a_2 \frac{1}{(2-y)} + a_3 \frac{y}{(2-y)}}{b_0 + b_1 n + b_2 \frac{1}{(2-y)} + b_3 \frac{y}{(2-y)}} \qquad 11)$$

a_0 – characterizes the main component of the reaction (NiO);

a_1 – refers to other components, the content of which in the mixture is determined by the stoichiometry of the chemical reaction (Li, O);

n is the coefficient of excess of the content of other components in relation to the main component; *n*=1 corresponds to the reaction stoichiometry. The coefficient *n* is always set for mixing the initial components of the reaction.
a_2 – determines the oxygen content in the reaction product;
a_3 – determines the oxygen content in the unspent balance of the original substance.

Let us discuss the possibilities of determining the coefficients a and b by fitting the experimental dependence $\frac{I_C}{I_R}(y)$. The experimental data show the values of *y* in the composition of the $Li_yNi_{2-y}O_2$ solid solution, obtained by the XRD method, as well as the ratio of the scattering peaks for mixtures of components, where the solid solutions $Li_yNi_{2-y}O_2$have concentration *y*. The numerator and denominator in formula (13) contain constant components, respectively, $(a_0 + a_1 \cdot n)$ and $(b_0 + b_1 \cdot n)$, which do not depend on *y* and are determined by the tabular values of the incoherent scattering function *S* and the squares of the atomic form factor f^2. Dependences of the second $\frac{1}{(2-y)}$ and the third $\frac{y}{(2-y)}$ terms on *y* are sharply different, which ensures the fitting of the experimental dependence $\frac{I_C}{I_R}(y)$.

3.2. Determination of the reaction mechanism

Consider the ternary system NiO-Li_2CO_3-NiO_2. Initial mixture for the reaction is $NiO + n \cdot \frac{1}{2}Li_2CO_3$. The reaction is described by the equation:

$$NiO + n \cdot \tfrac{1}{2} \cdot \tfrac{y}{(2-y)} Li_2CO_3 + \tfrac{1}{4} \cdot \tfrac{(y+4y')}{(2-y)} O_2 \downarrow = \tfrac{1}{(2-y)} \left(Li_yNi_{2-y-y'}O_2 + y'NiO_2\right) + \tfrac{y}{(2-y)} CO_2 \uparrow \quad (12)$$

The rest of the solid products after obtaining a solid solution:

$$Li_2CO_3 \cdot \left\{n - \frac{y}{(2-y)}\right\} \cdot \frac{1}{2} + \frac{1}{2-y} \cdot \left\{Li_yNi_{2-y-y'}O_2 + y'NiO_2\right\}$$

Then for Compton scattering we have:

$$S = S_{Ni} + n\left(S_{Li} + \tfrac{1}{2}S_C + \tfrac{3}{2}S_O\right) + \tfrac{2}{2-y} \cdot S_0 + \tfrac{2y'}{(2-y)}S_0 - \tfrac{y}{(2-y)}\left(\tfrac{3}{2}S_0 + \tfrac{1}{2}S_C\right) \quad (13)$$

Similarly for Rayleigh scattering:

$$f^2 = f_{Ni}^2 + n\left(f_{Li}^2 + \tfrac{1}{2}f_C^2 + \tfrac{3}{2}f_O^2\right) + \tfrac{2}{2-y} \cdot f_O^2 + \tfrac{2y'}{(2-y)}f_O^2 - \tfrac{y}{(2-y)}\left(\tfrac{3}{2}f_O^2 + \tfrac{1}{2}f_C^2\right) \quad (14)$$

Substituting the numerical data from Table 5 and grouping the terms, we obtain the dependence of the ratio of scattering peaks on two variables y and y'.

$$\frac{I_C}{I_R}(y,y') = \frac{\left(20.08+n\cdot16.16+\frac{(1-y')}{(2-y)}\cdot14.00-\frac{y}{(2-y)}\cdot13.22\right)}{\left(43.35+n\cdot3.20+\frac{(1-y')}{(2-y)}\cdot3.45-\frac{y}{(2-y)}\cdot3.12\right)} \quad (15)$$

A similar consideration for the *NiO-LiO₂– NiO₂* system:

$$\frac{I_C}{I_R}(y,y') = \frac{\left(20.08+n\cdot6.44+\frac{(1-y')}{(2-y)}\cdot14.00-\frac{y}{(2-y)}\cdot3.50\right)}{\left(43.35+n\cdot0.94+\frac{(1-y')}{(2-y)}\cdot1.73-\frac{y}{(2-y)}\cdot0.86\right)} \quad (16)$$

Table 5

Values of the atomic form factor *f* and incoherent scattering function *S* at $\frac{\sin\theta}{\lambda} = 1.08 Å^{-1}$ for chemical elements in the reaction of lithium nickelate formation according to J.H. Hubbell

Element	Li	C	O	Ni
f	0.277	1.033	1.376	6.584
S	2.942	5.434	7.002	20.088

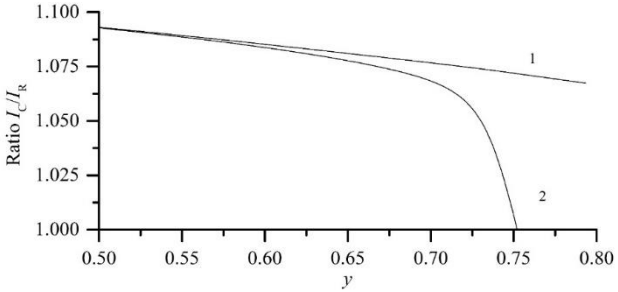

Fig. 7. Theoretical dependence of the ratio $\frac{I_C}{I_R}(y)$according to formula (15) with a smooth (curve1) and sharp (curve 2) change in the content y' of the NiO_2 phase in a mixture of components

Curve 1: $y' = (1-y)$; $\frac{I_C}{I_R}(y,y') = \frac{\left(20.08+n\cdot6.443+\frac{14}{(2-y)}\cdot14.00-3.50\cdot\frac{y}{(2-y)}+4.25\cdot\chi(y)\right)}{(43.35)}$

Curve 2: $y' = (1-y)\cdot\chi(y)$; $\frac{I_C}{I_R}(y,y') = \frac{\left(20.08+n\cdot6.443+\cdot14.00\cdot\chi(y)-3.50\cdot\frac{y}{(2-y)}\right)}{(43.35)}$

From a comparison of formulas (13) and (14) it follows that the coefficient at y' characterizes only scattering on oxygen (S_O and f_O^2). If the amount of NiO_2 changes little during the reaction ($y' \approx const$), then formula (15) gives a smooth dependence on y, shown in Fig. 7 (curve 1). With a sharp change in y', i.e. when the content of NiO_2changes, a feature should appear in the smooth dependence $\frac{I_C}{I_R}(y, y')$, (Fig. 7, curve 2).

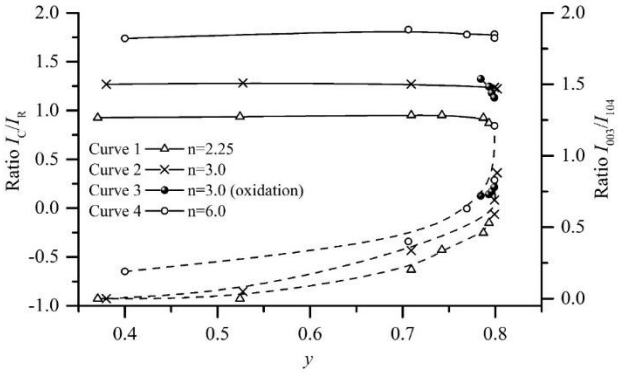

Fig. 8. Experimental dependences of the ratio of the peaks of Compton and Rayleigh scattering $\frac{I_C}{I_R}(y)$, as well as the ratio of the intensities of diffraction reflections $\frac{I_{(003)}}{I_{(104)}}$ (highlighted by a dotted line) on the content y of lithium in the solid solution $Li_yNi_{2-y}O_2$. Synthesis temperature is 650°C

A sharp change in the smooth dependence is observed on all experimental curves $\frac{I_C}{I_R}(y, y')$, however, the magnitude of the jump is different under different synthesis conditions (Fig. 8, 9). This sharp change occurs near $y \approx 0.78$, and the Δy range in which such a change occurs can be extremely small $\Delta y \approx 0.1$ (Fig. 9).

We fit the theoretical curve to describe such a sharp decline using the Heaviside function in the form:

$$\left(\frac{1}{\left(1+exp\left(-k(y-y_0)\right)\right)} - \frac{1}{\left(1+exp\left(-k(y-y^*)\right)\right)}\right), \qquad (17)$$

where $k = \frac{10}{\Delta x}$; Δy is the recession interval; $y^*$is an adjustment parameter for determining the position of the fall. For $y < y^*$, this function is equal to one, and then abruptly drops to zero in the interval Δy.

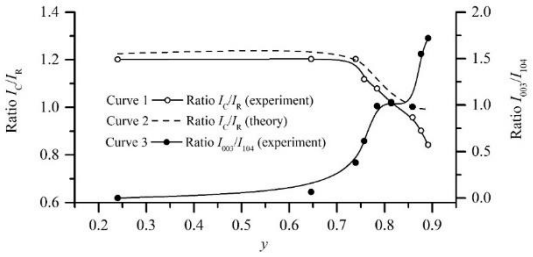

Fig. 9. Complex nature of dependences of the ratio of scattering peaks $\frac{I_C}{I_R}(y)$ and the ratio of diffraction peaks $\frac{I_{(003)}}{I_{(104)}}$ on the lithium content in the *y* range from 0.7 to 0.9. Synthesis temperature is 750°C. Excess lithium $n = 3.0$.

Figures 8 and 9 show fittings of the experimental curves $\frac{I_C}{I_R}(y, y')$ using the Heaviside function. We used the representation, $y' = p \cdot 2S_0$ and $y' = p \cdot 2f_0^2$, respectively, for the numerator and denominator of formulas (15) and (16). The parameter p characterizes the proportion of residual NiO_2 that has changed in the reagent system.

3.3. Determination of quantitative changes in the reagent system during intercalation

A sharp change in the experimental dependence $\frac{I_C}{I_R}(y)$ is accompanied by a sharp increase in the ratio of diffraction peaks $\frac{I_{(003)}}{I_{(104)}}$, which characterizes the intercalation process. With various technological processes, the parameter p characterizing the consumed amount of NiO_2, can vary from 0.30 (Fig. 8, curve 1) to 1.0 (Fig. 9, curve 2). In the first case, the ratio $\frac{I_{(003)}}{I_{(104)}}$ reaches 0.53, and in the second case, it is 1.72, which indicates a significant difference in the level of intercalation. Thus, the intercalation of $Li_yNi_{2-y}O_2$ is accompanied by a sharp decrease in the content of NiO_2 in the reagent system.

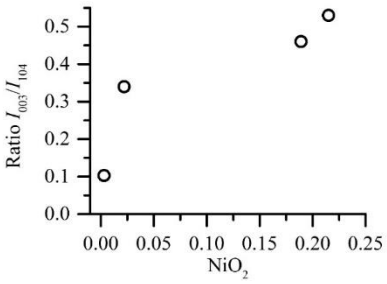

Fig. 10. The ratio of diffraction peaks $\frac{I_{(003)}}{I_{(104)}}$ depending on the consumption y' of the NiO_2 phase in the mixture of components

The decrease in the amount of residual NiO_2 in the system of reagents can be interpreted from the point of view of the supply of trivalent nickel to $Li_yNi_{2-y}O_2$ during intercalation. Fig. 10 shows the dependence of the amount of residual NiO_2 i.e. y', on the ratio $\frac{I_{(003)}}{I_{(104)}}$, which characterizes the ordering of the crystal lattice during intercalation. As follows from the data in Fig. 8, the degree of ordering of the solid solution lattice increases with increasing consumption of NiO_2. It can be concluded that it is this phase that is the supplier of trivalent nickel during intercalation. However, the value of the parameter p = 0.3, obtained by fitting the experimental curve, indicates that only 30% of the NiO_2 phase was consumed, and the intercalation process stopped.

We tried to initiate the process of supplying trivalent nickel by increasing n, which is the excess of the content of Li_2O or Li_2CO_3 relative to the stoichiometric value at a process temperature of 650°C. We did not observe any increase in the jump on the curve $\frac{I_C}{I_R}(y)$ up to n=6 (Fig. 8). We managed to increase the $\frac{I_{(003)}}{I_{(104)}}$ ratio to 0.78 for n=3; and for n=6 – even up to 1.2. However, it turned out to be impossible to exceed the value $y = 0.8$ of the lithium content in the solid solution. Thus, we cannot obtain $Li_yNi_{2-y}O_2$ with y value close to unity and the ratio $\frac{I_{(003)}}{I_{(104)}} \approx 1.3 \div 1.5$ (P. Kalyani et al.) at temperature 650°C. An increase in the consumption of NiO_2 (an increase in the value of p in the fitting curve) was achieved by forced oxidation of the mixture in the «boat». Curve 3 (red) in Fig.8 shows a fivefold increase in the jump in the range of $y = 0.78 \div 0.8$. By fitting the experimental curve, the value $p \approx 0.5$ was obtained compared to $p = 0.12$ (curve 2) for the original curve. However, such an increase in the consumption of NiO_2 did not lead to

a significant increase in the degree of lattice ordering. Indeed, after a fifty-hour annealing, the $\frac{I_{(003)}}{I_{(104)}}$ ratio remained at the level of ≈ 0.7.

In conclusion, we note that the supply of trivalent lithium during intercalation can be controlled by the magnitude of the jump in the $\frac{I_C}{I_R}(y)$ dependences. However, this process is not directly related to structural ordering, which is characterized by the ratio $\frac{I_{(003)}}{I_{(104)}}$.

3.4. The effect of temperature on the supply of trivalent nickel during intercalation

An increase in temperature to 750°C leads to the decomposition of Li_2CO_3 (T=720°C) into Li_2O and CO_2 (P. Kalyani et al.), and for any source of lithium, the reaction $NiO + n \cdot \frac{1}{2} Li_2O$ is allowed. For this reaction, the ratio of the peaks of coherent and incoherent scattering is described by relation (16). The experimental curve $\frac{I_C}{I_R}(x)$ (Fig. 9) drops sharply in the y range from 0.63 to 0.89. There are two decline segments 0.63÷0.81 and 0.87÷0.89 in this range of y. The entire curve and the first section of the decline are well fitted by relation (16) and give the value $p = 1$. This means that all NiO_2 has already been consumed at $y \approx 0.8$. A further increase in y corresponds to the transition of the figurative point to another area of the diagram. It is noteworthy that the $\frac{I_{(003)}}{I_{(104)}}$ ratio does not increase with increasing y in the y range from 0.78 to 0.86, which indicates that the ordering process stops when the NiO_2 source in the reactant mixture is depleted.

Further ordering of the structure of the solid solution $Li_yNi_{2-y}O_2$, which is observed in the y range from 0.87 to 0.89 by the increase in the $\frac{I_{(003)}}{I_{(104)}}$ ratio, is also accompanied by a sharp decrease in the ratio $\frac{I_C}{I_R}$. However, in our opinion, it is not associated with the consumption of the NiO_2 source and the supply of trivalent nickel.

3.5. Some conclusions about the mechanism of lithiation-oxidation of NiO

At the beginning of the process, there is a monotonic change in both the lithium content y in the solid solution and the effective atomic number of the mixture of components. The change in the $\frac{I_C}{I_R}$ ratio is quite consistent with the basic reactions (3) up to $y \approx 0.7$. In the y range 0.7÷0.8, there is a sharp change in this ratio, which is accompanied by an increase in the intensity of the superstructural reflection (003). An increase in the (003) reflection intensity indicates the ordering of the $Li_yNi_{2-y}O_2$ crystal lattice upon intercalation. In accordance with model calculations using formulas (14) and

(15), a sharp change in the $\frac{I_C}{I_R}$ ratio indicates a change in the amount of the NiO_2 phase in the reactant mixture. According to the literature data, this phase serves as a source of trivalent nickel, which enters the intercalation zone.

Reducing the amount of NiO_2 depends on the technological conditions of the process. At a temperature of 650°C, which is lower than the decomposition temperature of Li_2CO_3 (T=720°C), it is not possible to achieve complete consumption of the NiO_2 phase: the consumption coefficient p is at the level of 0.15 (see explanation to the formula (15)), and only the forced oxidation of the reactant mixture made it possible to increase p to 0.5. At the same time, the content y of lithium in the solid solution could not be raised above $y = 0.8$.

The degree of ordering the $Li_yNi_{2-y}O_2$ lattice, characterized by the ratio $\frac{I_{(003)}}{I_{(104)}}$, was increased to 1.21 by enriching the initial mixture of components with lithium. However, it was not possible to obtain $LiNiO_2$ with the given characteristics of $y = 1$ and $\frac{I_{(003)}}{I_{(104)}} = 1.3 \div 1.5$. It can be concluded that the supply of trivalent nickel from NiO_2 and the ordering of $Li_yNi_{2-y}O_2$ lattice are two processes that should be considered independently.

CONCLUSIONS

High-temperature synthesis of layered structures $Li_yNi_{2-y}O_2$ includes three main stages: (1) consumption of a lithium source (Li_2CO_3); (2) saturation of NiO nanoparticles with lithium to form a disordered solid solution $Li_yNi_{2-y}O_2$; (3) ordering of the solid solution with formation of a layered structure. Each of these stages may turn out to be limiting and determine the kinetics of synthesis as a whole, and, consequently, the quality of the final product. The use of a set of X-ray methods made it possible to experimentally study the kinetics of each stage depending on the synthesis temperature and the amount of excess of the lithium-containing phase in comparison with the stoichiometric composition. The need for an excess in lithium is due to its uncontrolled exit outside the reaction volume during high-temperature synthesis and is provided for in most technological modes. Consumption of the lithium-source phase at a synthesis temperature of 650 °C, i.e. below the melting point of Li_2CO_3 (T = 720 °C) is described by a linear time dependence, which is typical for a zero-order reaction. At a synthesis temperature of 750°C, the kinetic curve is described by an exponential dependence; this dependence is typical for a first-order reaction, which can be associated with the decomposition of Li_2CO_3 molecules. In both cases, it was experimentally established that the greater the Li_2CO_3 excess, the more its blocks enlarge during synthesis. This leads to an experimentally observed decrease in the rate of the Li_2CO_3 source consumption, since the smaller the nanoparticle size, the higher their chemical activity.

The kinetic curves *y(t)* for the formation of the $Li_yNi_{2-y}O_2$ solid solution generally correspond to diffusion kinetics. No differences in the rate of the process with different excess of lithium have been observed. However, a tendency towards asymptotic exit of the curves to the values of y for equilibrium phases $Li_{0.75}Ni_{1.25}O_2$ and $LiNiO_2$ is detected. The kinetic curves of the ordering process, $I_{003}/I_{104}(t)$, are piecewise linear, but contain areas with zero slope. The linearity corresponds to zero-order reactions.The rate of these reactions depends in different ways on the excess of lithium at different synthesis temperatures.

In solid-phase synthesis (T = 650°C), the ordering rate increases with an increase in the excess of lithium, and does not change with a molten source (T = 750°C). This means that, during solid-phase synthesis, the rate of intercalation of lithium ions into the $Li_yNi_{2-y}O_2$ lattice increases with an increase in its excess in the mixture. When the molten Li_2CO_3 phase surrounds the $Li_yNi_{2-y}O_2$ particles (Chung-Hsin Lu et al.), the excess of the lithium-containing phase does not affect the intercalation rate.

Taking into account the complexity of these processes, the empirical development of the optimal synthesis technology is practically impossible. Knowing the quantitative ratios of the rates of these three high-temperature processes of $Li_yNi_{2-y}O_2$ synthesis, it is possible to calculate the optimal technological mode: temperature, excess of the lithium-containing phase, the size of nano-blocks in NiO and the lithium source phase, etc. For a preliminary assessment of the effect of the kinetics of processes on the final product, we propose an experimental «composition-ordering» diagram. This diagram allows you to determine the displacement of the phase space point, which is due to the kinetics of the processes, relative to the equilibrium curve.

Based on the results of this work, it is possible to state general practical recommendations for the technology of obtaining a nano-scale $Li_yNi_{2-y}O_2$ solution:

1) use of NiO and the lithium source with nano-size structural elements; 2) use of the lowest possible synthesis temperature (T < 720°C); 3) keep the excess of lithium-containing phases at least 5 mass% at synthesis temperature.

We believe that taking into account the kinetics of these processes will give a possibility to accurately select the temperature and excess lithium to obtain a given state of the final product.

SUMMARY

In this work, for the first time, two X-ray methods are jointly applied for the physicochemical analysis of the process: XRD and the ratio of the peaks of coherent and incoherent scattering. XRD provides information about the phases in a mixture of components and the structure of a solid solution, but does not allow one to determine the composition of a mixture of chemical elements with a small atomic number.

The ratio of the scattering peaks together with the XRD data makes it possible to determine the trajectory of the figurative point from the phase diagram. Fitting is carried out using model calculations of the dependence $\frac{I_C}{I_R}(y)$ for hypothetical chemical reactions. Such calculations are quite similar to mass balance calculations, in which instead of the mass of individual chemical compounds, the values of the incoherent scattering functions and the squares of the atomic form factor are used. Such calculations can be performed for any given chemical reaction and are comparable with the experimental dependence of the ratio of scattering peaks for a mixture of components during the reaction. For the process of lithiation-oxidation of NiO, using such calculations, it was possible to establish that two processes dominate during intercalation: the ordering of the solid solution lattice and the supply of trivalent nickel to the intercalation zone. These two processes are basically independent and are determined by different technological parameters. It has been empirically shown that in order to obtain $LiNiO_2$ with good electrochemical properties, it is necessary not only to obtain the composition $LiNiO_2$, but also to ensure the ratio of structural reflections $I(003)/I(104)$ in the range of 1.3–1.5. This paper shows that this can be done only by varying different technological parameters of the process, namely: the amount of excess lithium, forced oxidation of the mixture of components and temperature. To control the production of single-phase $LiNiO_2$, one XRD method is not enough. There is no certainty in the complete absence of foreign phases in the final product if the exact position of the figurative point of this product on the phase diagram is unknown.

The very important process of supplying trivalent nickel is difficult to control by XRD. It should be estimated from the ratio of scattering peaks using the calculation of model chemical reactions. Thus, to obtain $LiNiO_2$ with high electrophysical properties, it is necessary to control three processes: the formation of the $Li_yNi_{2-y}O_2$ solid solution, its ordering during intercalation, and the supply of trivalent nickel.

Bibliography

1. P. Kalyani, N. Kalaiselvi, Sci. Technol. Adv. Mater, 2005, 6(6), pp. 689-703. https://doi.org/10.1016/j.stam.2005.06.001

2. M. Bianchini, Angew. Chem. Int. Ed., 2018, 58(31). DOI: 10.1002/anic.201812472

3. P. Barton, D. Premchand, P. Chater, R. Seshadri, M. Rosseinsky, Chem. Euro. J. 2013, 19, 14521. https://doi.org/10.1002/chem.201301451

4. T. Ohzuki, A. Veda, M. Nagayam, Electrochem. Acta, 1993, 38 p. 1159.

5. S. Deng, L. Xue, Y. Li, Z. Lin, W. Li, Y. Chen, T. Lei, J. Zhu, J. Zhang, J. Fuel Cell Sci. Technol., 2019, 16(3). DOI: 10.1115/1.4042552

6. Chung-Hsin Lu, Lee Wei-Cheng, J. Mater. Chem, 2000, 10, pp. 1403-1407. https://doi.org/10.1039/A909130K
7. V. Kaplan, E. Wachtel, I. Lubomirsky, J. Chem. Thermodyn, 2011, 43(11), pp.1623-1627. https://doi.org/10.1016/j.jct.2011.05.020
8. D. Gonzalez-Varela, H. Pfeiffer B. Alcántar-Vázquez, Journal of Materiomics, 2018, 4(1), pp.56-61. DOI: 10.1016/j.jmat.2017.12.004
9. B. Delmon, Introduction a la Cinetique Heterogene. Edition Technip. 7 Rue Nelaton, Paris, 1969, p. 540.
10. I.F. Mikhailov, A.A. Baturin, A.I. Mikhailov, S.S. Borisova, L.P. Fomina, Rev. Sci. Instrum, 2018, 89(2), 023103, DOI:10.1063/1.4993101
11. P. Duvauchell, Nucl. Instrum. Methods Phys. Res., Sect. B, 1999, 155, pp. 221-228
12. J.H. Hubbell, Phys. Chem. Ref. Data. 1975, 4, p. 471 https://doi.org/10.1063/1.555523
13. Mikhailov I.F., Gabielkov S.V., Mikhailov A.I., Surovitskiy S.V., Rev. Sci. Instrum., 2022, 93, 084102 DOI: 10.1063/5.0089144
14. Hena Das, Chem. Mater, 2017, 29(18) pp. 7840-7851 https://doi.org/10.1021/acs.chemmater 7b02546
15. T. Karakasidis and M. Meyer, Phys.Rev B, 1997, 55(20), pp. 13853-13864
16. C. D'Agostino, Chem. Eng. Sci., 2012, 74, pp. 105-113.
17. R.V. Moshtev, P. Zatilova, V.Menev, A.Sato, J. Power Sources, 1993, 54, p. 329.
18. H. Migeon et al. The Li2O– NiO -O2 system at 670°C, J. Materials Science, 13, 1978, p.461-466
19. S.Pizzini, R.Morlotti, V.Wagner, J.Electrochem.Soc 116(7), 915 (1969)

Information about the authors:
Mikhailov Igor Fedorovych,
Doctor of Physical and Mathematical Sciences,
Chief Researcher at the Department of Physics of Metals and Semiconductors
National Technical University «Kharkov Polytechnic Institute»
2, Kyrpychova str., 61002 Kharkiv, Ukraine

Mikhailov Anton Igorovych,
Doctor of Physical and Mathematical Sciences,
Leading Researcher at the Department of Physics of Metals and Semiconductors
National Technical University «Kharkov Polytechnic Institute»
2, Kyrpychova str., 61002 Kharkiv, Ukraine